



**HAL**  
open science

## **Ionothermal synthesis of calcium-based metal–organic frameworks in a deep eutectic solvent**

Michaël Teixeira, Renata Maia, Lydia Karmazin, Benoît Louis, Stéphane Baudron

► **To cite this version:**

Michaël Teixeira, Renata Maia, Lydia Karmazin, Benoît Louis, Stéphane Baudron. Ionothermal synthesis of calcium-based metal–organic frameworks in a deep eutectic solvent. *CrystEngComm*, 2022, 24 (3), pp.601-608. 10.1039/D1CE01497H . hal-03705540

**HAL Id: hal-03705540**

**<https://hal.science/hal-03705540>**

Submitted on 28 Jun 2022

**HAL** is a multi-disciplinary open access archive for the deposit and dissemination of scientific research documents, whether they are published or not. The documents may come from teaching and research institutions in France or abroad, or from public or private research centers.

L'archive ouverte pluridisciplinaire **HAL**, est destinée au dépôt et à la diffusion de documents scientifiques de niveau recherche, publiés ou non, émanant des établissements d'enseignement et de recherche français ou étrangers, des laboratoires publics ou privés.

## **Ionothermal synthesis of calcium-based metal-organic frameworks in a deep eutectic solvent**

Michaël Teixeira,<sup>a</sup> Renata A. Maia,<sup>a</sup> Lydia Karmazin,<sup>b</sup> Benoît Louis\*<sup>c</sup> and Stéphane A. Baudron\*<sup>a</sup>

<sup>a</sup> *Université de Strasbourg, CNRS, CMC UMR 7140, 4 rue Blaise Pascal, F-67000 Strasbourg, France. E-mail : [sbaudron@unistra.fr](mailto:sbaudron@unistra.fr)*

<sup>b</sup> *Fédération Chimie Le Bel, FR 2010, BP296R8, 1 rue Blaise Pascal, F-67008 Strasbourg cedex, France.*

<sup>c</sup> *Université de Strasbourg, CNRS, ICPEES UMR 7515, 25 rue Becquerel, F-67087 Strasbourg, France. E-mail : [blouis@unistra.fr](mailto:blouis@unistra.fr)*

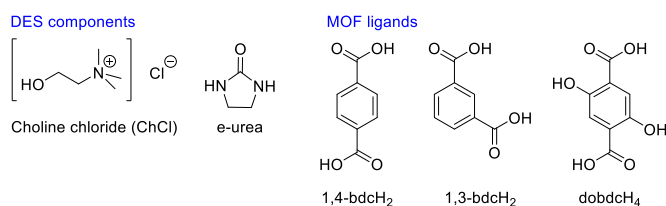
The unprecedented use of a deep eutectic solvent (DES) for the ionothermal synthesis of Ca(II) based metal-organic frameworks (MOFs) has been explored. The 1:2 choline chloride:e-urea DES (e-urea = 2-imidazolidinone, ethylene urea) has been successfully employed for the preparation of Ca-MOFs with a series of dicarboxylic acid ligands. These materials have been structurally characterized by single-crystal and powder X-ray diffraction as well as by thermogravimetric analysis, infra-red, UV-visible and emission spectroscopies in the crystalline state. The MOFs obtained have been found to be three-dimensional with the presence of channels occupied by coordinated e-urea solvent molecules. While the latter solvent acts as a bridging ligand in the case of the terephthalate and isophthalate based MOFs, it behaves as a terminal ligand in the MOFs isolated with the 2,5-dihydroxyterephthalate (dobdcH<sub>2</sub><sup>2-</sup>). With this ligand, two phases differing in the coordination mode of the dobdcH<sub>2</sub><sup>2-</sup> anion have been obtained. Interestingly, for one of them formulated [Ca(dobdcH<sub>2</sub>)(e-urea)<sub>2</sub>], the crystals rapidly lost their transparency and luster upon exposure to air. This phenomenon could be rationalized by X-ray diffraction to result from the uptake of water molecule from ambient atmosphere leading to the replacement of one e-urea molecule by a H<sub>2</sub>O in the Ca(II) cation coordination sphere. These results demonstrate that the 1:2 choline chloride:e-urea DES can be considered as an effective solvent for the synthesis of water-sensitive Ca-MOFs.

### **Introduction**

Metal-Organic Frameworks (MOFs) represent an important class of crystalline porous materials with diverse applications such as in gas storage and separation, heterogeneous catalysis or optics.<sup>1-3</sup> Built from the assembly of organic ligands with metal nodes, the properties of MOFs are determined by the nature of these components and their structural arrangement. While the vast majority of these materials is constructed using transition metal or rare earth cations, recent efforts have been devoted to the use of s-block ions<sup>4-8</sup> with a particular emphasis on alkaline earth metals such as Ca(II).<sup>9-10</sup> Indeed, it is an inexpensive naturally abundant element, has a lower toxicity and features low density, particularly favourable for gas sorption. These interesting characteristics of Ca-based MOFs come with a catch, since the coordination number and geometry of this cation are harder to predict and its oxophilicity makes it prone to coordination by water molecules at the expense of ligand binding, potentially leading

to architectures of low dimensionality. Therefore, the solvothermal approach is the preferred synthetic method over the hydrothermal one, to prevent competing coordination by water, although synthesis based on water/solvent combinations have been reported.<sup>7-10</sup> Surprisingly, to the best of our knowledge and according to a recent review,<sup>10</sup> there have been no reports of Ca-MOFs prepared following the ionothermal strategy, in spite of its appealing characteristics for such purposes.<sup>11-15</sup>

This methodology is based on the use of an ionic environment to act as solvent and template for the formation of MOFs. First applied to ionic liquids, its use has been extended to deep eutectic solvents (DESs). The latter are an emerging class of synthetic media resulting from mixing two or more species, in an appropriate ratio, which are usually solids and prone to hydrogen bonding. This mixture yields a fluid with a freezing temperature below the one of either component. DESs have low vapor pressure, relatively wide liquid range, non-flammability, the ability to dissolve polar species, limited toxicity and an improved biocompatibility, as they may be composed of naturally occurring compounds.<sup>16-23</sup> DESs are thus adequate solvents for MOF synthesis but they also impact the material formation in diverse ways.<sup>11-15</sup> Components of the solvent may be coordinated to the metal centers or be present within the pores of the MOFs<sup>24</sup> and the 1:2 combinations of choline chloride (ChCl) with urea derivatives have been shown to induce the conversion from one MOF structure to another and to affect the crystal morphology and textural properties.<sup>25</sup> Furthermore, DESs allow the formation of MOFs comprising metal-halide bonds normally prone to hydrolysis.<sup>25,26</sup> It has been proposed that, as in ionic liquids,<sup>27-30</sup> water potentially present in these solvents is molecularly dispersed or distributed in small aggregates and that the interaction with the anions of the DES lowers the water nucleophilicity.<sup>26</sup> This feature may be of relevance to the formation of Ca-MOFs of higher dimensionality and the absence of such literature precedent is thus striking. In this context, we have investigated the use of these solvents for the synthesis of Ca-MOFs with a variety of dicarboxylic acid ligands (Scheme 1) and demonstrate herein their applicability for such purpose including for water-sensitive systems.



**Scheme 1.** Representations of the DES components and MOF ligands employed in this study.

## Results and discussion

Both the 1:2 ChCl:urea solvent, known as reline,<sup>31</sup> and the ChCl:e-urea (1:2) DES<sup>32</sup> (e-urea = 2-imidazolidinone, ethylene urea, Scheme 1) were explored as media for MOF synthesis. However, only microcrystalline powders were obtained in reline and no single crystal structure determination by X-ray diffraction could be performed. Contrastingly, in the e-urea based system, a series of crystalline materials were isolated and characterized as discussed hereafter.

**Table 1** Crystallographic data for Ca-MOFs **1-5**.

	<b>1</b>	<b><math>\alpha</math>-2</b>	<b><math>\beta</math>-2</b>	<b>3</b>	<b>4</b>	<b>5</b>
Formula	C <sub>22</sub> H <sub>20</sub> Ca <sub>2</sub> N <sub>4</sub> O <sub>10</sub>	C <sub>11</sub> H <sub>10</sub> CaN <sub>2</sub> O <sub>5</sub>	C <sub>22</sub> H <sub>20</sub> Ca <sub>2</sub> N <sub>4</sub> O <sub>10</sub>	C <sub>11</sub> H <sub>10</sub> CaN <sub>2</sub> O <sub>7</sub>	C <sub>14</sub> H <sub>16</sub> CaN <sub>4</sub> O <sub>8</sub>	C <sub>28</sub> H <sub>34</sub> Ca <sub>2</sub> N <sub>8</sub> O <sub>17</sub>
FW	580.58	290.29	580.58	322.29	408.39	834.79
Crystal system	triclinic	orthorhombic	monoclinic	triclinic	monoclinic	triclinic
Space group	<i>P</i> -1	<i>P</i> 2 <sub>1</sub> 2 <sub>1</sub> 2 <sub>1</sub>	<i>P</i> 2 <sub>1</sub> / <i>n</i>	<i>P</i> -1	<i>C</i> 2/ <i>c</i>	<i>P</i> -1
<i>a</i> / Å	7.0098(2)	6.7109(3)	6.8835(4)	8.4045(10)	17.7069(8)	10.628(2)
<i>b</i> / Å	10.9304(3)	10.2710(4)	17.9272(11)	8.6975(9)	10.4537(8)	13.310(3)
<i>c</i> / Å	16.6160(5)	17.7750(7)	20.4957(13)	9.8540(13)	9.3801(6)	13.741(3)
$\alpha$ / °	92.6180(10)			64.455(3)		79.741(6)
$\beta$ / °	99.6590(10)		90.043(3)	86.316(4)	92.379(4)	73.155(6)
$\gamma$ / °	102.7040(10)			74.126(4)		71.586(5)
<i>V</i> / Å <sup>3</sup>	1219.82(6)	1225.19(9)	2529.2(3)	623.92(13)	1734.78(19)	1757.0(6)
<i>Z</i>	2	4	4	2	4	2
<i>T</i> / K	173(2)	173(2)	173(2)	173(2)	173(2)	120(2)
$\mu$ / mm <sup>-1</sup>	0.533	0.530	0.514	0.542	0.415	0.413
Refls. coll.	30448	26052	49825	8071	17536	48159
Ind. refls. ( <i>R</i> <sub>int</sub> )	6646 (0.0476)	3622 (0.0692)	7333 (0.0901)	3376 (0.0555)	2564 (0.0584)	8378 (0.1248)
<i>R</i> <sub>I</sub> ( <i>I</i> >2 $\sigma$ ( <i>I</i> )) <sup>a</sup>	0.0325	0.0594	0.0550	0.0637	0.0367	0.1062
<i>wR</i> <sub>2</sub> ( <i>I</i> >2 $\sigma$ ( <i>I</i> )) <sup>a</sup>	0.0777	0.1396	0.1364	0.1680	0.0940	0.2921
<i>R</i> <sub>I</sub> (all data) <sup>a</sup>	0.0401	0.0688	0.0788	0.0904	0.0419	0.1592
<i>wR</i> <sub>2</sub> (all data) <sup>a</sup>	0.0821	0.1436	0.1487	0.1819	0.0982	0.3345
<i>GOF</i>	1.045	1.199	1.065	1.093	1.064	1.051

<sup>a</sup>  $R_1 = \sum ||F_o| - |F_c|| / \sum |F_o|$ ;  $wR_2 = [\sum w(F_o^2 - F_c^2)^2 / \sum wF_o^4]^{1/2}$ .

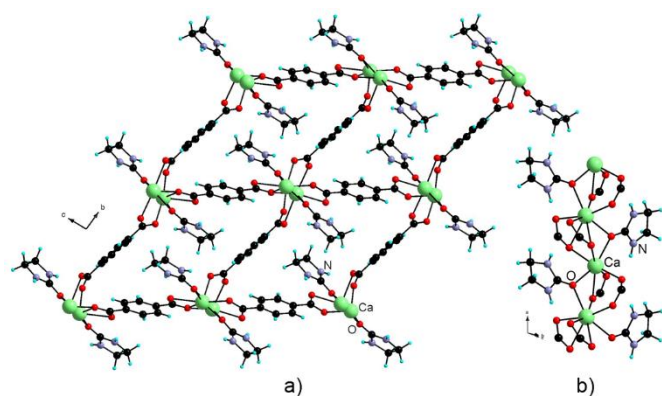


**Fig. 1.** View along the *a* axis of the crystal structure of Ca-MOF **1** (a) and of the details of the metal-organic chain where only the carboxylate moieties are shown for clarity (b).

Upon heating a 1:2 mixture of 1,4-bdcH<sub>2</sub> (terephthalic acid, 1,4-benzenedicarboxylic acid, Scheme 1) and Ca(NO<sub>3</sub>)<sub>2</sub>·4H<sub>2</sub>O in the e-urea based DES at 140°C for 10 days, white crystals of Ca-MOF **1** were obtained in 94% yield. Compound **1** formulated [Ca<sub>2</sub>(1,4-bdc)<sub>2</sub>(e-urea)<sub>2</sub>] crystallizes in the triclinic *P*-1 space group (Table 1). The two crystallographically independent Ca(II) cations are octa-coordinated, bound each to four bridging carboxylic acid groups of (1,4-bdc)<sup>2-</sup> ligands and to the carbonyl oxygen atom of two e-urea molecules (Fig. 1 and Table 2). This results in the formation of 1D metal-organic chains that upon bridging by the terephthalate dianions leads to a 3D organization with channels along the *a* axis (Fig. 1). Within this secondary building unit, the Ca(II) cations are distant of 3.5320(4)-3.7031(4) Å, while the shortest distance between alkaline earth centers between consecutive chains is 9.2405(5) Å. This overall 3D arrangement is reminiscent of the one observed in other Ca-1,4-bdc MOFs such as [Ca(1,4-bdc)(DMF)(H<sub>2</sub>O)] or [Ca<sub>3</sub>(1,4-bdc)(nmp)<sub>2</sub>] (nmp = 1-methyl-2-pyrrolidinone).<sup>33,34</sup> However, it is worth noting that in these materials the solvent molecules act as terminal ligands and are not bridging in contrast with the structure of **1**.

**Table 2.** Selected distances (Å) in the different secondary building units and shortest distance between the Ca(II) cations of different chains bridged by the dicarboxylate ligands.

	Ca- O <sub>carboxylic</sub>	Ca-O <sub>e-urea</sub>	Ca-Ca <sub>SBU</sub>	Ca- Ca <sub>chains</sub>
<b>1</b>	2.2969(11)- 2.6662(11)	2.3929(10)- 2.4278(10)	3.5320(4)- 3.7031(4)	9.2405(5)
<b>α-2</b>	2.332(4)- 2.595(4)	2.401(3)- 2.417(4)	3.488(1)	9.518(1)
<b>β-2</b>	2.292(3)- 2.901(3)	2.398(3)- 2.521(3)	3.5107(11)- 3.5785(11)	9.5127(9)
<b>3</b>	2.303(2)- 2.755(3)	2.294(3)	4.152(1)- 5.334(1)	6.467(1)
<b>4</b>	2.2978(11)- 2.3518(10)	2.3044(12)	4.873(1)	10.281(1)
<b>5</b>	2.271(5)- 2.384(4)	2.318(5)- 2.326(5)	4.830(2)- 5.155(2)	9.795(2)

Powder X-ray diffraction analyses demonstrated that Ca-MOF **1** is the main crystalline phase (see Fig. S1 ESI). Elemental analysis confirmed the chemical purity of the material. Thermogravimetric analysis indicated that the material is stable up to 350°C where a weight loss corresponding to the two e-urea molecules is observed (see Fig. S2 ESI), associated with a loss of crystallinity, preventing further investigation of the sorption properties. The diffuse reflectance spectrum of Ca-MOF **1** (Fig. S4 ESI) shows a broad band with a maximum at ca. 290 nm. Upon excitation at this wavelength, a weak emission is observed at 345 nm (Fig. S5 ESI), consistent with what has been reported for other Ca(1,4-bdc) MOFs.<sup>33</sup>

When performing the same reaction with 1,3-bdcH<sub>2</sub> (isophthalic acid, 1,3-benzenedicarboxylic acid, Scheme 1) at 120°C, a mixture of two Ca-MOFs,  $\alpha$ -**2** and  $\beta$ -**2**, was obtained (Fig. 2). These two compounds are formulated [Ca(1,3-bdc)(e-urea)]<sub>n</sub> (n = 1, 2) and are polymorphs. MOF  $\alpha$ -**2** crystallizes as twinned transparent blocks in the *P*2<sub>1</sub>2<sub>1</sub>2<sub>1</sub> orthorhombic space group. The Ca(II) cation exhibits an eightfold coordination, bound to carboxylate groups and e-urea molecules (Fig. 2b and Table 2), similarly to what is observed in the structure of **1** (Fig. 1b). This leads to 1D chains that are bridged by isophthalate dianions affording a 3D arrangement with channels along the *a* axis. The shortest Ca-Ca distance within the secondary building unit is 3.488(1) Å and 9.518(1) Å between chains. Interestingly,  $\alpha$ -**2** is isostructural to [Ca(1,3-bdc)(pyr)] (pyr = 2-pyrrolidinone), where the solvent only differs by the presence of a methylene group in place of one NH.<sup>34</sup> This MOF has been obtained by heating a mixture of the ligand and Ca(NO<sub>3</sub>)<sub>2</sub>·4H<sub>2</sub>O in pure 2-pyrrolidinone at 190°C for 6 days.<sup>34</sup>

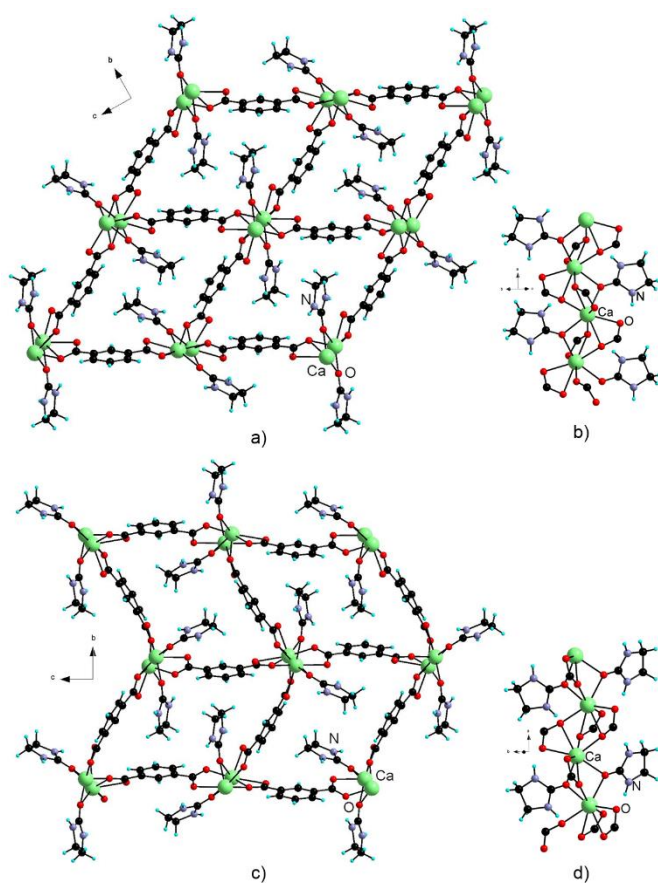


**Fig. 2.** View along the *a* axis of the crystal structure of Ca-MOFs  $\alpha$ -**2** (a) and  $\beta$ -**2** (c) and of the respective secondary building units (b) and (d) for which only the carboxylate moieties are shown for clarity.



Polymorph  $\beta$ -2 crystallizes in the  $P2_1/n$  monoclinic space group with two crystallographically independent Ca(II) cations, two 1,3-bdc<sup>2-</sup> anions and two e-urea molecules in the asymmetric unit. Both Ca(II) cations are eight-coordinated. However, the organization of the coordinating moieties within the secondary building unit differs from the one in  $\alpha$ -2 with an alternation of the combination of two e-urea molecules and one carboxylate group on one hand, and three carboxylate groups on the other hand (Fig. 2d and Table 2). Here again, a 3D organization featuring channels along the  $a$  crystallographic axis is observed (Fig. 2c). X-ray powder diffraction of the crystal batches confirmed the presence of both  $\alpha$ -2 and  $\beta$ -2 phases (see Fig. S6 ESI). We have been unable so far to produce exclusively one of the two MOFs and have consistently obtained this mixture of polymorphs, preventing further investigation of their properties. Investigation by TGA indicated that these compounds exhibit a thermal profile similar to the one of **1** (see Fig. S7 ESI).

The use of the dobdcH<sub>4</sub> ligand (2,5-dihydroxyterephthalic acid, Scheme 1) was then explored. This ligand is of interest as it forms the series of MOF-74<sup>35</sup> also known as CPO-27<sup>36</sup> materials formulated M<sub>2</sub>(dobdc) that has been described with a wide series of divalent metal cations, including Mg(II)<sup>37</sup> but not with Ca(II). Upon heating a 1:2 mixture of dobdcH<sub>4</sub> and Ca(NO<sub>3</sub>)<sub>2</sub>·4H<sub>2</sub>O in the e-urea based DES at 140°C for 10 days, a mixture of two crystalline phases was obtained. The major compound crystallized as yellowish needles in the  $P-1$  triclinic space group (Table 1) and is formulated [Ca(dobdcH<sub>2</sub>)(e-urea)], **3** (Fig. 3). The asymmetric unit of this 3D MOF consist of one Ca(II) cation, two dobdcH<sub>2</sub><sup>2-</sup> anions on inversion centers and one e-urea molecule. The alkaline earth metal center is coordinated to seven oxygen atoms belonging to either the e-urea molecule acting here as a terminal ligand, the carboxylate or the hydroxyl groups of the dobdcH<sub>2</sub><sup>2-</sup> anions (Fig. 3, Table 2). In this respect, it can be noted that the two crystallographically independent bridging ligands show different coordination modes. While one is bound to the Ca(II) centers solely via the carboxylate moieties (Fig. 3c), the other one also involves the OH groups (Fig. 3d). This type of coordination has been observed in other Ca-MOFs,<sup>33,38</sup> and actually compound **3** is isostructural to [Ca(dobdcH<sub>2</sub>)(DMF)] that has been prepared from a DMF/EtOH/H<sub>2</sub>O (7/2/1) mixture at pH = 3 upon heating at 120°C for 2 days.<sup>33</sup>

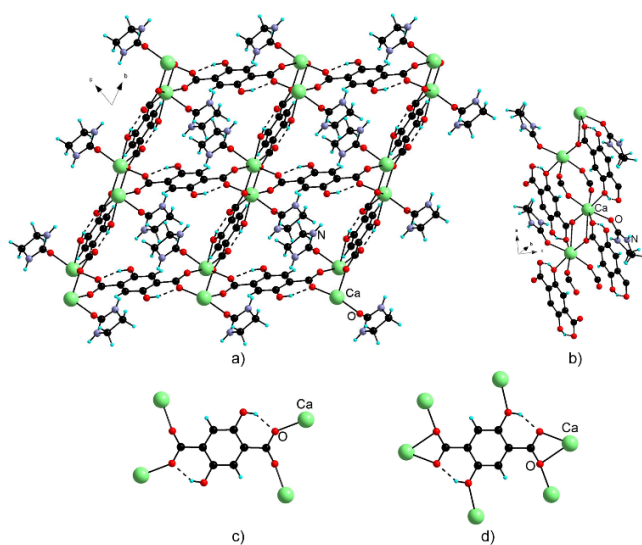


**Fig. 3.** View along the  $a$  axis of the crystal structure of Ca-MOF **3** (a), the secondary building unit (b) and the two modes of coordination of the two crystallographically independent dobdcH<sub>2</sub><sup>2-</sup> ligands (c and d).

Along with **3**, large prismatic yellow crystals of **4** (see Fig. S9 in ESI) were isolated as a minor product. Ca-MOF **4** formulated  $[\text{Ca}(\text{dobdcH}_2)(\text{e-urea})_2]$ , crystallizes in the monoclinic  $C2/c$  space group (Table 1) with one Ca(II) cation, one dicarboxylate anion and one e-urea molecule in the asymmetric unit. The metal center adopts an octahedral coordination geometry with four carboxylate groups and two e-urea molecules in *cis* position (Fig. 4a and 4b, Table 2). Unlike in the structure of **3**, the hydroxyl groups are here not involved in the coordination. The distance between consecutive Ca(II) centers in **3** and **4** are significantly longer than in **1**,  $\alpha$ -**2** and  $\beta$ -**2** where the carbonyl oxygen atom is coordinated in a  $\mu$  fashion. Bridging by the dicarboxylate ligands leads to a 3D organization with channels along the *c* axis ( $d_{\text{Ca-Ca}} = 10.281 \text{ \AA}$ ) occupied by the coordinated e-urea molecules (Fig. 4a). This MOF is isostructural to  $[\text{Ca}(\text{dobdcH}_2)(\text{solvent})_2]$  (solvent = dimethylformamide or *N,N*-dimethylacetamide).<sup>33,39</sup>

Interestingly, a peculiar behaviour of crystals of **4** could be noticed. Indeed, upon exposure of the material to air, the crystals rapidly lost their transparency and luster (see Fig. S10 ESI). Interestingly, the XRD powder pattern of a sample obtained by grinding one large single crystal of **4** showed the gradual conversion of this material to another phase, **5**, upon exposure to air over several days (Fig. 5, Fig. S11 ESI). Although the crystals of **4** crack and break into very small pieces in the course of the aging process (see Fig. S10 ESI), single-crystal X-Ray diffraction data collection on one such fragment could be performed, allowing the structure determination of the transformed material, **5** (Table 1).

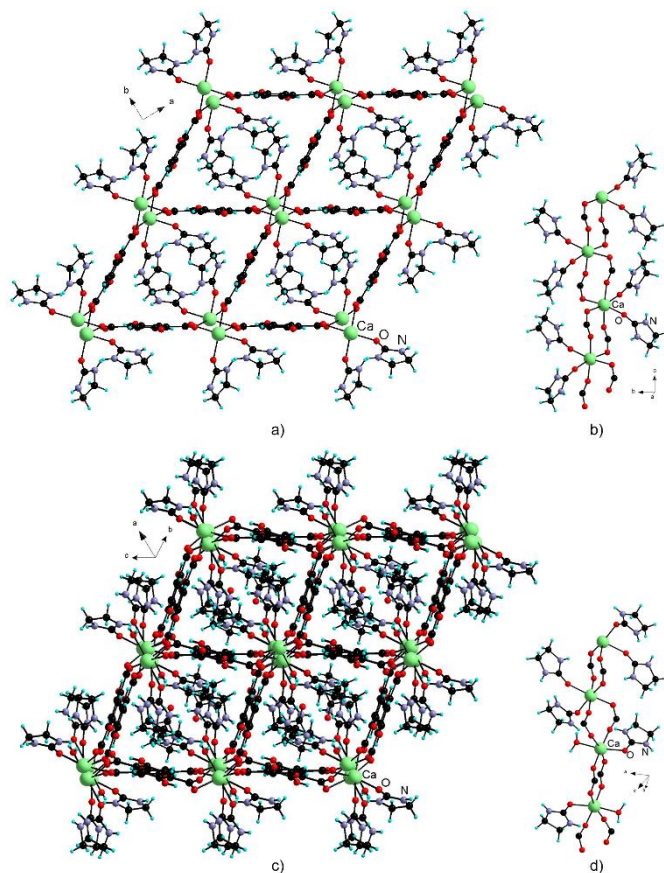


**Fig. 4.** Views of the crystal structure of 3D Ca-MOF **4** and **5** (a and c) and of the respective metal-ligand chains (b and d). For the latter representation, only the carboxylate moieties of the  $\text{dobdcH}_2^{2-}$  anion are shown for clarity.



Ca-MOF **5** formulated  $[\text{Ca}_2(\text{dobdcH}_2)_2(\text{e-urea})_3(\text{H}_2\text{O})](\text{e-urea})$  crystallizes in the *P*-1 triclinic space group (Fig. 4c). It is based on two crystallographically independent Ca(II) cations that are both in an octahedral environment as they are coordinated to four bridging carboxylate groups and either two terminal e-urea molecule (as in **4**) or an e-urea and a water molecule (Fig. 4d). Therefore, it appears that a water molecule has substituted in *trans* position an e-urea, and the latter is consequently present unbound in the channels of the 3D architecture. The crystal structure of **5** may be regarded as a snapshot of the transformation of **4** upon water exposure. This phenomenon differs from the reported conversion of  $[\text{Ca}(\text{dobdcH}_2)(\text{DMF})_2]$  into  $[\text{Ca}(\text{dobdcH}_2)(\text{H}_2\text{O})_2]$  via a dissolution/reorganization process by immersion of MOF crystals in a MeOH/H<sub>2</sub>O (95/5).<sup>33</sup> In this case, a complete exchange was described. In the present case, it is noteworthy that, since e-urea is not volatile, it remains in the channels of the MOF when removed from the coordination sphere of the Ca(II) centers and that the exchange happens solely via exposure to ambient air via a mechanism that still remains to be determined. It can also be inferred from this observation that the DES allows the formation of a Ca-MOF, **4**, that is otherwise water sensitive. Therefore, the ChCl:e-urea (1:2) DES is an efficient solvent for the preparation of 3D MOFs without undesired coordination of water molecule and even for moisture sensitive materials.

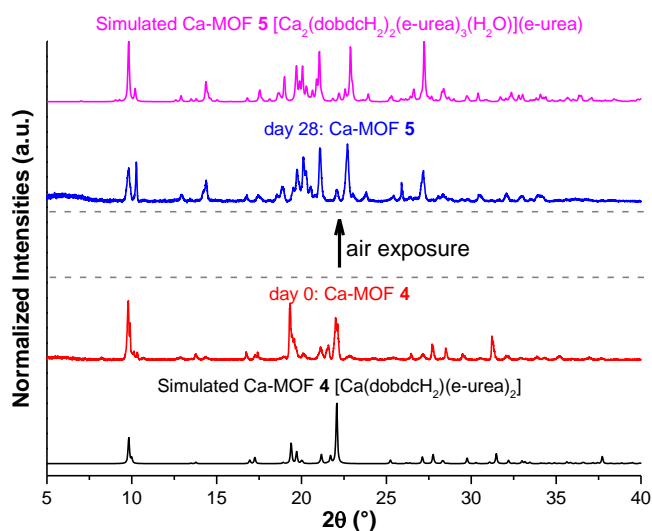


**Fig. 5.** Time evolution of the powder X-ray diffraction pattern of **4** upon exposure to air showing the conversion to **5**. Note that the simulated pattern for **4** is based on single-crystal data collected at 173 K and the one for **5** on data collected at 120 K, while experimental data has been collected at room temperature.

The diffuse reflectance spectra of Ca-MOFs **3**, **4** and **5** feature a broad band with a maximum around 380-400 nm for the three compounds (Fig. S14 ESI). Interestingly, the luminescence spectra of these MOFs upon excitation at 390 nm differ strongly (Fig. 6). While a broad emission centered at 570 nm is observed for **3**, it is centered at 495 nm for **4** and **5**. One possible explanation for this hypsochromic shift may be found in the different coordination modes of the ligand when comparing the materials. Indeed, it has been recently rationalized for  $(\text{dobdcH}_2)^{2-}$  based MOFs with alkaline earth metals<sup>39</sup> that two possible ligand-centered emitting states co-exist: one resulting from relaxation of the S<sub>1</sub> excited state and the other corresponding to relaxation from a lower lying excited state formed after excited state intramolecular proton

transfer (ESIPT).<sup>40</sup> It has been proposed that the relative contribution of either state is impacted by temperature, the nature of the metal cation as well as by the coordination mode. Binding of the metal center to the hydroxyl group of the ligand assists the ESIPT and may favour contribution of the relaxation from this lower energy state to the emission.<sup>39</sup> Consistently, a lower energy emission is observed for **3** for which the Ca cation is coordinated to the carboxylate groups and to the hydroxyl group (Fig. 3), in contrast to Ca-MOFs **4** and **5** featuring solely binding to the carboxylate moieties (Fig. 4).

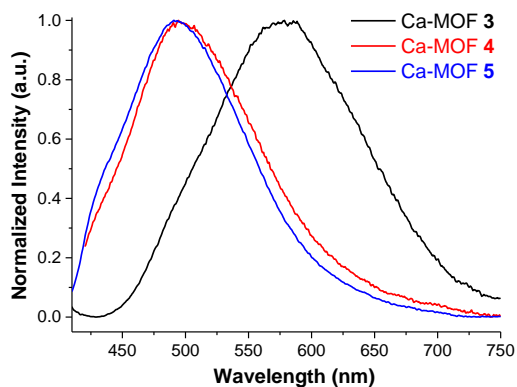


**Fig. 6.** Solid state emission spectra of Ca-MOFs **3-5** upon excitation at 390 nm at room temperature.

## Conclusions

The 1:2 choline chloride:e-urea DES (e-urea = 2-imidazolidinone, ethylene urea) has been successfully employed for the preparation of Ca-MOFs with a series of dicarboxylic acid ligands that could be characterized by single-crystal X-ray diffraction. The structure determination of these materials showed a three-dimensional arrangement with the presence of channels occupied by coordinated e-urea molecules. While the latter solvent acts as a bridging ligand in the case of the terephthalate and isophthalate based MOFs, **1** and  $\alpha/\beta$ -**2** respectively, it behaves as a terminal ligand in the MOFs isolated with the 2,5-dihydroxyterephthalate ( $\text{dobdcH}_2^{2-}$ ). With this ligand, two phases, **3** and **4**, differing in the coordination mode of the  $\text{dobdcH}_2^{2-}$  anion have been concomitantly obtained. This difference in ligand binding mode may be at stake in the varying emission properties of these MOFs. Indeed, **3** involving coordination of both the carboxylate and hydroxyl groups shows a lower energy emission than **4**,  $\lambda_{\text{em}} = 575$  vs 495 nm upon excitation at 390 nm.

Interestingly, the crystals of **4** rapidly lost their transparency and luster upon exposure to air, converting to another phase **5** as indicated by the evolution of the XRD powder pattern over several days. This phenomenon could be rationalized by single-crystal X-ray diffraction to result from the uptake of water molecule from ambient atmosphere leading to the replacement of one e-urea molecule by  $\text{H}_2\text{O}$  in the Ca(II) cation coordination sphere and its subsequent release inside the pores of the MOF.

The foregoing results demonstrate that the 1:2 choline chloride:e-urea DES can not only be considered as an alternative to solvents such as DMF or N,N-dimethylacetamide, commonly used for Ca-MOF synthesis, but also that it allows the preparation of materials exhibiting water

sensitivity. Future work will focus on the use of this DES with other alkaline earth metals as well as other bridging ligands towards the formation of porous materials.

## Experimental section

### Synthesis

The DES was freshly prepared before each synthesis by heating at 100°C a 1:2 mixture of ChCl and e-urea placed in a round-bottom flask, until formation of a homogeneous liquid phase.

**Ca-MOF 1, Ca(1,4-bdc)(e-urea):** Terephthalic acid, 1,4-bdcH<sub>2</sub>, (0.199 g, 1.2 mmol) and Ca(NO<sub>3</sub>)<sub>2</sub>·4H<sub>2</sub>O (0.567 g, 2.4 mmol) were added to a 20 mL vial before addition of freshly prepared choline chloride:e-urea 1:2 DES (15 mL). The vial was then heated at 140°C for 10 days. After completion of the reaction and before letting the vial cool down, ethanol was added to prevent solidification. The resulting mixture was then filtered and washed multiple times with small amounts of ethanol. The remaining solid was air-dried to afford **1** as a white crystalline solid (0.328 g, 94.2%). Elemental analysis (CHN) for C<sub>11</sub>H<sub>10</sub>CaN<sub>2</sub>O<sub>5</sub> ([Ca(1,4-bdc)(e-urea)]), calculated: C, 45.51; H, 3.47; N, 9.65; found: C, 44.92; H, 3.64; N, 9.90.

**Ca-MOFs  $\alpha$ -2 and  $\beta$ -2, [Ca(1,3-bdc)(e-urea)]<sub>n</sub>:** Following the same procedure with isophthalic acid, 1,3-bdcH<sub>2</sub>, (0.199 g, 1.2 mmol) and Ca(NO<sub>3</sub>)<sub>2</sub>·4H<sub>2</sub>O (0.567 g, 2.4 mmol) at 120°C, a mixture of  $\alpha$ -2 and  $\beta$ -2 was obtained (0.216 g, 62.0%). Elemental analysis (CHN) for C<sub>11</sub>H<sub>10</sub>CaN<sub>2</sub>O<sub>5</sub> ([Ca(1,3-bdc)(e-urea)]), calculated: C, 45.51; H, 3.47; N, 9.65; found: C, 45.05; H, 3.69; N, 10.33.

**Ca-MOFs 3 and 4, [Ca(dobdcH<sub>2</sub>)(e-urea)] and [Ca(dobdcH<sub>2</sub>)(e-urea)<sub>2</sub>]:** Following the same procedure as for **1** using 2,5-dihydroxyterephthalic acid, dobdcH<sub>4</sub>, (0.238 g, 1.2 mmol) and Ca(NO<sub>3</sub>)<sub>2</sub>·4H<sub>2</sub>O (0.567 g, 2.4 mmol) at 140°C, a mixture of **3** and **4** was obtained as small yellow needles and large prismatic crystals respectively (0.184 g). Elemental analysis (CHN) for C<sub>11</sub>H<sub>10</sub>CaN<sub>2</sub>O<sub>7</sub> ([Ca(dobdcH<sub>2</sub>)(e-urea)]), calculated: C, 40.99; H, 3.13; N, 8.69; found: C, 39.28; H, 3.87; N, 10.09.

Upon exposure of crystals of **4** to air, Ca-MOF **5** formed by uptake of water over several days. After 28 days: Elemental analysis (CHN) for C<sub>28</sub>H<sub>34</sub>Ca<sub>2</sub>N<sub>8</sub>O<sub>17</sub> ([Ca<sub>2</sub>(dobdcH<sub>2</sub>)<sub>2</sub>(e-urea)<sub>3</sub>(H<sub>2</sub>O)](e-urea)), calculated: C, 40.29; H, 4.10; N, 13.42; found: C, 40.21; H, 4.24; N, 13.85.

### X-ray diffraction

For Ca MOFs **1-4**, Data (Table 1) were collected at 173 K on a Bruker SMART CCD diffractometer with Mo-K $\alpha$  radiation. Both structures were solved using SHELXS-97 and refined by full matrix least-squares on  $F^2$  using SHELXL-2016 with anisotropic thermal parameters for all non-hydrogen atoms.<sup>41</sup> The hydrogen atoms were introduced at calculated positions and not refined (riding model). For Ca-MOF **5**, X-ray diffraction data collection was carried out at 120 K on a Bruker PHOTON III DUO CPAD diffractometer equipped with an Oxford Cryosystem liquid N<sub>2</sub> device, using Mo-K $\alpha$  radiation ( $\lambda = 0.71073$  Å). The crystal-detector distance was 37 mm. The cell parameters were determined (APEX3 software)<sup>42</sup> from reflections taken from 1 set of 180 frames at 1 s exposure. The structure was solved using the program SHELXT-2014.<sup>43</sup> The refinement and all further calculations were carried out using SHELXL-2014.<sup>41</sup> The hydrogen atoms of the water molecule were located from the difference Fourier map. The other H-atoms were included in calculated positions and treated as riding

atoms using SHELXL default parameters. The non-H atoms were refined anisotropically, using weighted full-matrix least-squares on  $F^2$ . A semi-empirical absorption correction was applied using SADABS in APEX3;<sup>42</sup> transmission factors:  $T_{\min}/T_{\max} = 0.6254/0.7456$ .

X-ray diffraction powder patterns were recorded at 293 K on a Bruker D8 diffractometer using monochromatic Cu-K $\alpha$  radiation with a scanning range between 4 and 40° using a scan step of 0.0225°/min. The simulated diagrams were generated with the Mercury® software based on the single-crystal data collected.

### **Thermo-gravimetric analysis**

The thermal stability of the samples was accessed in a PerkinElmer Thermogravimetric Analyzer TGA 4000 under N<sub>2</sub> flow of 20 mL/min, and a heating rate of 5°C/min up to 800°C.

### **Optical properties**

Diffuse reflectance spectra were collected on a PerkinElmer Lambda 650S UV-Vis spectrometer at room temperature. Emission spectra were collected on a PerkinElmer LS55 fluorescence spectrometer.

### **Elemental analysis**

Elemental analyses (CHN) were performed at the Service Commun d'Analyses of the University of Strasbourg, in duplicate, employing a ThermoFischer Flash 2000 equipment, whereas the reported values for the CHN were taken as the average of two measurements.

### **Author Contributions**

Investigation: M. T., R. A. M., L. K., S. A. B.; methodology: M. T., R. A. M. and S. A. B.; writing – original draft: S. A. B.; writing – review & editing: M. T., L. K., R. A. M. and B. L.; funding acquisition: B. L. and S. A. B.

### **Conflicts of interest**

There are no conflicts to declare.

### **Acknowledgements**

This work has benefited from support provided by the University of Strasbourg Institute of Advanced Study (USIAS), within the French national programme “Investment for the future” (IdEx-Unistra). We also thank the Université de Strasbourg, the C.N.R.S., and the Ministère de l'Enseignement Supérieur, de la Recherche et de l'Innovation for financial support.

### **References**

- 1 H. C. Zhou, J. R. Long and O. M. Yaghi, *Chem. Rev.*, 2012, **112**, 673-674, Metal-organic frameworks special issue.
- 2 H. C. J. Zhou and S. Kitagawa, *Chem. Soc. Rev.*, 2014, **43**, 5415-5418, themed issue on metal-organic frameworks.
- 3 M. Dincă and J. R. Long, *Chem. Rev.*, 2020, **120**, 8037-8038, Porous framework chemistry special issue.

- 4 Q.-G. Zhai, X. Bu, X. Zhao, C. Mao, F. Bu, X. Chen and P. Feng, *Cryst. Growth Des.*, 2016, **16**, 1261-1267.
- 5 Q.-G. Zhai, X. Bu, C. Mao, X. Zhao, L. Daemen, Y. Cheng, A. J. Ramirez-Cuesta and P. Feng, *Nat. Commun.*, 2016, **7**, 13645.
- 6 X. Zhao, M. S. Shimazu, X. Chen, X. Bu and P. Feng, *Angew. Chem. Int. Ed.*, 2018, **57**, 6208-6211.
- 7 D. Banerjee and J. B. Parise, *Cryst. Growth Des.*, 2011, **11**, 4704-4720.
- 8 M. A. Alnaqbi, A. Alzamly, S. H. Ahmed, M. Bakiro, J. Kegere and H. L. Nguyen, *J. Mater. Chem. A*, 2021, **9**, 3828-3854.
- 9 Y. Zang, L.-K. Li and S.-Q. Zang, *Coord. Chem. Rev.*, 2021, **440**, 213955.
- 10 S. Xian, Y. Lin, H. Wang and J. Li, *Small*, 2021, **17**, 2005165.
- 11 E. Parnham and R. E. Morris, *Acc. Chem. Res.*, 2007, **40**, 1005-1013.
- 12 R. E. Morris, *Chem. Commun.*, 2009, 2990-2998.
- 13 B. Zhang, J. Zhang and B. Han, *Chem. Asian J.*, 2016, **11**, 2610-2619.
- 14 P. Li, F.-F. Cheng, W.-W. Xiong and Q. Zhang, *Inorg. Chem. Front.*, 2018, **5**, 2693-2708.
- 15 R. A. Maia, B. Louis and S. A. Baudron, *CrystEngComm*, 2021, **23**, 5016-5032.
- 16 Q. Zhang, K. de Oliveira Vigier, S. Royer and F. Jérôme, *Chem. Soc. Rev.*, 2012, **41**, 7108-7146.
- 17 C. Russ and B. König, *Green Chem.* 2012, **14**, 2969-2982.
- 18 M. Francisco, A. van den Bruinhorst and M. C. Kroon, *Angew. Chem. Int. Ed.*, 2013, **52**, 3074-3085.
- 19 E. L. Smith, A. P. Abbott and K. S. Ryder, *Chem. Rev.*, 2014, **114**, 11060-11082.
- 20 B. Gurkan, H. Squire and E. Pentzer, *J. Phys. Chem. Lett.*, 2019, **10**, 7956-7964.
- 21 M. A. R. Martins, S. P. Pinho and J. A. P. Coutinho, *J. Sol. Chem.*, 2019, **48**, 962-982.
- 22 B. B. Hansen, St. Spittle, B. Chen, D. Poe, Y. Zhang, J. M. Klein, A. Horton, L. Adhikari, T. Zelovich, B. W. Doherty, B. Gurkan, E. J. Maginn, A. Ragauskas, M. Dadmun, T. A. Zawodzinski, G. A. Baker, M. E. Tuckerman, R. F. Savinell and J. R. Sangoro, *Chem. Rev.*, 2021, **121**, 1232-1285.
- 23 D. Yu, Z. Xue and T. Mu, *Chem. Soc. Rev.*, 2021, **50**, 8596-8638.
- 24 J. Zhang, T. Wu, S. Chen, P. Feng and X. Bu, *Angew. Chem. Int. Ed.*, 2009, **48**, 3486-3490.
- 25 R. A. Maia, B. Louis and S. A. Baudron, *Dalton Trans.*, 2021, **50**, 4145-4151.
- 26 E. A. Drylie, D. S. Wragg, E. R. Parnham, P. S. Wheatley, A. M. Z. Slawin, J. E. Warren and R. E. Morris, *Angew. Chem. Int. Ed.*, 2007, **46**, 7839-7843.

- 27 L. Cammarata, S. G. Kazarian, P. A. Salter and T. Welton, *Phys. Chem. Chem. Phys.*, 2001, **3**, 5192-5200.
- 28 C. G. Hanke and R. M. Lynden-Bell, *J. Phys. Chem. B*, 2003, **107**, 10873-10878.
- 29 Y. Yasaka, C. Wakai, N. Matubayashi and M. Nakahara, *J. Phys. Chem. A*, 2007, **111**, 541-543.
- 30 E. Amigues, C. Hardacre, G. Keane, M. Migaud and M. O'Neill, *Chem. Commun.*, 2006, 72-74.
- 31 A. P. Abbott, G. Capper, D. L. Davies, R. K. Rasheed and V. Tambyrajah, *Chem. Commun.*, 2003, 70-71.
- 32 E. R. Parnham, E. A. Drylie, P. S. Wheatley, A. M. Z. Slawin and R. E. Morris, *Angew. Chem. Int. Ed.*, 2006, **45**, 4962-4966.
- 33 P.-C. Liang, H.-K. Liu, C.-T. Yeh, C.-H. Lin and V. Zima, *Cryst. Growth Des.*, 2011, **11**, 699-708.
- 34 M. Kang, D. Luo, Y. Deng, R. Li and Z. Lin, *Inorg. Chem. Comm.*, 2014, **47**, 52-55.
- 35 N. L. Rosi, J. Kim, M. Eddaoudi, B. Chen, M. O'Keeffe and O. M. Yaghi, *J. Am. Chem. Soc.* 2005, **127**, 1504-1518.
- 36 P. D. C. Dietzel, R. E. Johnsen, R. Blom and H. Fjellvåg, *Chem. Eur. J.*, 2008, **14**, 2389-2397.
- 37 S. R. Caskey, A. G. Wong-Foy and A. J. Matzger, *J. Am. Chem. Soc.*, 2008, **130**, 10870-10871.
- 38 P. D. C. Dietzel, R. Blom and H. Fjellvåg, *Z. Anorg. Allg. Chem.*, 2009, **635**, 1953-1958.
- 39 A. Douvali, G. S. Papaefstathiou, M. Pia Gullo, A. Barbieri, A. C. Tsipis, C. D. Malliakas, M. G. Kanatzidis, I. Papadas, G. S. Armatas, A. G. Hatzidimitriou, T. Lazarides and M. J. Manos, *Inorg. Chem.*, 2015, **54**, 5813-5826.
- 40 J. Zhao, S. Ji, Y. Chen, H. Guo and P. Yang, *Phys. Chem. Chem. Phys.*, 2012, **14**, 8803-8817.
- 41 G. M. Sheldrick, *Acta Cryst.*, 2015, **C71**, 3-8.
- 42 "M86-EXX229V1 APEX3 User Manual", Bruker AXS Inc., Madison, USA, 2016.
- 43 G. M. Sheldrick, *Acta Cryst.*, 2015, **A71**, 3-8.